# Reconfigurable Dual-Stopband Filters With Reduced Number of Couplings Between a Transmission Line and Resonators

Kangho Lee, Tae-Hak Lee, *Student Member, IEEE*, Chang-Soo Ahn, Young-Sik Kim, *Member, IEEE*, and Juseop Lee, *Member, IEEE*

***Abstract*—This letter proposes a new design method for a bandstop filter with two stopbands. Contrary to a conventional method, the presented method allows for achieving two stopbands without increasing the number of the couplings between resonators and the transmission line connecting the input and output ports. In addition, a filter designed using the presented method can not only have different center frequencies but also have different bandwidths by adjusting the resonant frequencies of the resonators. For verification of the proposed approach a dual-stopband filter using four tunable substrate-integrated waveguide resonators has been designed and measured.**

***Index Terms*—Dual-stopband filter, reconfigurable filter, substrate-integrated resonator.**

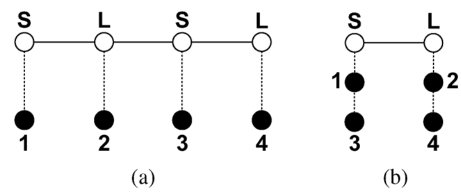


| | Proposed filter | Conventional filter |
|---|---|---|
| # of resonators | 4 | 4 |
| # of couplings between a TL and resonaotors | 2 | 4 |
| The minimum length of TL | λ/4 | λ/2 |

(c)

Fig. 1. Routing diagram of the 2nd-order dual-stopband filter (a) conventional dual-stopband filter (b) proposed dual-stopband filter (c) comparison between proposed topology and conventional one.

## I. Introduction

BANDSTOP filters have been widely used in wireless transceivers to suppress unwanted signals. Conventional design methods are well known and bandstop filters with Butterworth and Chebyshev responses can be designed by using the normalized lowpass lumped element values followed by applying the lowpass-to-bandstop frequency transformation [1], [2]. Another method is using the coupling matrices for resonator-coupled bandstop filters. Synthesis methods for the bandstop filter coupling matrices are presented and various bandstop filters designed by using the coupling matrices are described in [3]–[6].

Fundamental structures of the bandstop filters consist of a uniform transmission line(TL) and resonators [1], [7], [8]. The transmission line runs from the input port to the output port, and each resonator is coupled to the transmission line. Two stopbands can be established by cascading two bandstop filters. However, this method doubles the length of the transmission line and the transmission line experiences more couplings with the resonators. As the transmission line couples to the resonators, the characteristic impedance of the transmission line deviates from 50 Ω [9]. Hence, in designing the bandstop filter, it is preferred to reduce the number of the couplings between the transmission line and the resonators.

Hence, in this letter, we propose a method to obtain and adjust two stopbands for a tunable bandstop filter without increasing the number of the couplings between the transmission line and the resonators. Our demonstration begins with filter synthesis for obtaining a response with two symmetric Butterworth-response stopbands. We then describe that this response can be tuned to have asymmetric responses and/or equi-ripple responses by adjusting the resonant frequency of the resonators. For verifying the proposed method, we have designed and measured a dual-stopband filter.

## II. Filter Synthesis and Design

A conventional way to construct two reconfigurable stop-bands is cascading two frequency-agile bandstop filters. Fig. 1(a) shows an example of cascading two second-order bandstop filters. $S$ and $L$ represent the source and load, respectively, and the filled circles represent the resonators. The drawback of the conventional structure described in Introduction can be reduced by arranging the resonators in such a way that half of the resonators are coupled to the transmission line. For example, Fig. 1(b) shows that only two resonators are coupled to the transmission line. In this letter, we show a synthesis method for the dual-stopband filter with the topology shown in Fig. 1(b), and present methodologies for adjusting frequency responses.

Manuscript received July 29, 2014; revised October 24, 2014; accepted November 20, 2014. Date of publication January 09, 2015; date of current version February 10, 2015. This work was supported by the Agency for Defense Development (Contract number: UD120046FD) and by the Basic Science Research Program through the National Research Foundation of Korea (NRF) funded by the Ministry of Education, Science, and Technology (2012R1A1A1004665).

K. Lee, T.-H. Lee, Y.-S. Kim, and J. Lee are with Korea University, Seoul, Korea (phone: +82-2-3290-4848; e-mail: ifsnow@ieee.org).

C.-S. Ahn is with the 3rd. R&D Institute-2, Agency for Defence Development, Daejeon, Korea.

Color versions of one or more of the figures in this letter are available online at http://ieeexplore.ieee.org.

Digital Object Identifier 10.1109/LMWC.2014.2382659

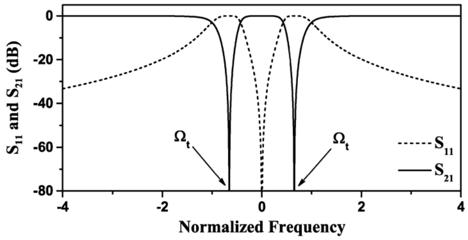


Fig. 2. Theoretical results of a symmetric Butterworth response in the normalized frequency domain.

In this work, we begin with synthesizing a dual-bandstop filter with a symmetric Butterworth response shown in Fig. 2. The frequency response shown in Fig. 2 has four transmission zeros. Two of them are at $S = -j\Omega_t = -j0.654$ and the others are at $S = j\Omega_t = j0.654$. Two reflection zeros are at $S = 0$, and the others are at $S = j\infty$ and $S = -j\infty$. With given transmission and reflection zeros, the transmission coefficient can be derived and it is given by

$$t(S) = \frac{P(S)}{\epsilon E(S)} = \frac{\sum p_m S^m}{\epsilon \left(\sum e_n S^n\right)} \tag{1}$$

where $S$ represents normalized complex frequency, and $\epsilon$ is the ripple factor.

The $(N+2) \times (N+2)$ normalized coupling matrix of the filter topology shown in Fig. 1(b) is given by

$$\mathbf{M} = \begin{bmatrix} 0 & M_{S,1} & 0 & 0 & 0 & M_{S,L} \\ M_{S,1} & M_{1,1} & 0 & M_{1,3} & 0 & 0 \\ 0 & 0 & M_{2,2} & 0 & M_{2,4} & M_{2,L} \\ 0 & M_{1,3} & 0 & M_{3,3} & 0 & 0 \\ 0 & 0 & M_{2,4} & 0 & M_{4,4} & 0 \\ M_{S,L} & 0 & M_{2,L} & 0 & 0 & 0 \end{bmatrix} \tag{2}$$

The transmission coefficient of the corresponding coupling matrix can be found by using

$$t(S) = 2(\mathbf{R} + S\mathbf{W} + j\mathbf{M})^{-1}_{6,1} \tag{3}$$

where $\mathbf{R}$ is a 6×6 matrix whose only nonzero elements are $\mathbf{R}_{1,1} = \mathbf{R}_{6,6} = 1$ and $\mathbf{W}$ is similar to the identity matrix except that $\mathbf{W}_{1,1} = \mathbf{W}_{6,6} = 0$[10].

The coupling matrix can be obtained by using both (1) and (3), and the entries of the matrix are found to be

$$\begin{aligned} M_{S,L} &= 1 \\ M_{S,1} &= M_{2,L} = \sqrt{e_3} = 0.900 \\ M_{1,3} &= M_{2,4} = \sqrt[4]{p_0} = \Omega_t = 0.654 \\ M_{1,1} &= M_{2,2} = M_{3,3} = M_{4,4} = 0 \end{aligned} \tag{4}$$

It is worth noting that the coupling coefficients can be found analytically with ease from $e_3$ and $\Omega_t$.

The frequency response of the topology having the normalized coupling values in (4) is shown in Fig. 2. It is worth noting that the coupling matrix is synthesized in such a way that the 3 dB points ranges from $-1$ to $+1$ in the normalized frequency domain. This bandwidth corresponds to the design bandwidth used in actual filter design in actual frequency domain. According to (4), inter-resonator coupling, $M_{1,3} = M_{2,4}$, determines transmission zero, $\Omega_t$. Hence, the separation between two stopbands can be changed by adjusting inter-resonator coupling.

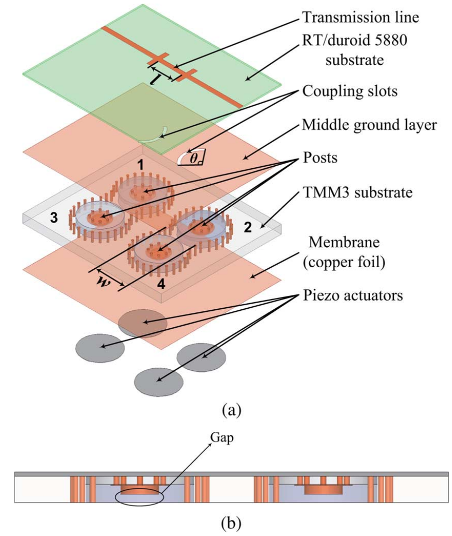


Fig. 3. 3D-view of the designed filter (a) layer-by-layer structure ($\boldsymbol{l} = 9$ mm, $\boldsymbol{w} = 11.2$ mm, $\theta = 104°$) (b) side-view. The gap between the post and the membrane is exaggerated and some of via-holes are not shown for the reader's convenience. The resonant frequency of each resonator can be controlled by adjusting this gap by means of a piezo actuator whose deflection range limits the tuning range of each resonator.

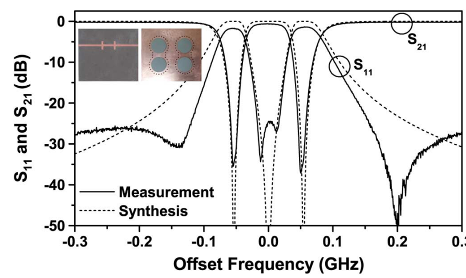


Fig. 4. Synthesized and measured results of symmetric Butterworth response.

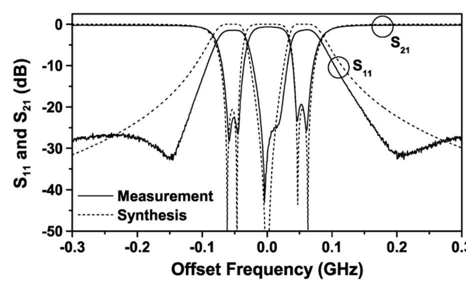


Fig. 5. Synthesized and measured results of symmetric equi-ripple response.

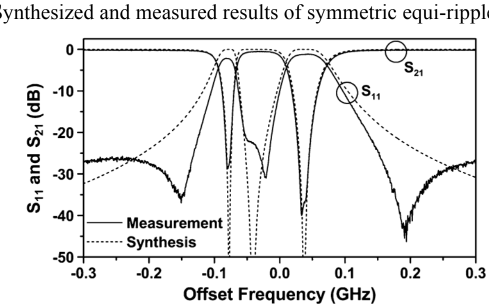


Fig. 6. Synthesized and measured results of asymmetric Butterworth response.

To verify the proposed topology, a dual-stopband filter has been designed using substrate-integrated frequency tunable cavity resonators. For demonstration, the center frequency and

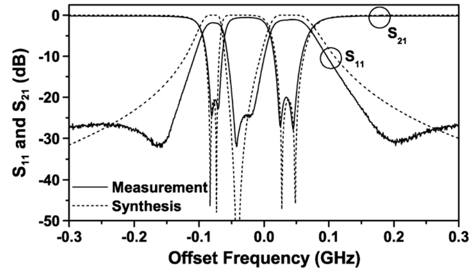


Fig. 7. Synthesized and measured results of asymmetric equi-ripple response.

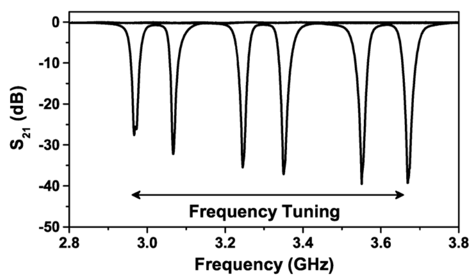


Fig. 8. Measured results with different center frequencies.

design bandwidth have been arbitrary defined to be 3.3 GHz and 165 MHz, respectively. Since, the substrate-integrated frequency tunable cavity resonator has been used in bandstop filter designs [5], [6], [9], its properties and design method are not repeated in this letter. Fig. 3 shows a 3-D layer-by-layer structure and a side-view of the designed filter. Numbers marked in Fig. 3(a) depict the number of the resonators. The transmission line between the resonators 1 and 2 is 90° long and each resonator is established by via holes whose radius is 0.35 mm. The radius of the cavity is designed to be 8 mm and the diameter of the post located at the center of each resonator is 4.6 mm. The cavities are embedded in 3.175 mm thick Rogers TMM3 substrate and the transmission line is fabricated on 0.508 mm thick RT/duroid 5880 substrate. The microstrip transmission line and patchs are shown in Fig. 3(a).

The external coupling structures are realized by coupling slots between the transmission line and the resonators, and the inter-resonator coupling structures are implemented by inductive irises. The dimensions of the coupling structure can be determined by the methods described in [11]and [8], and they are given in Fig. 3.

## III. Measurement and Reconfigurability

The filter has been fabricated and measured for verification of the presented bandstop filter topology. Fig. 4 shows the measured and synthesized symmetric Butterworth responses and its inset shows the fabricated filter. The measured results exhibit attenuation larger than 35 dB at each stopband. The discrepancy between the synthesized and measured responses of $S_{11}$ mainly due to the presence of the additional reflection zeros can be attributed to frequency-dependent characteristic of the transmission line [12]. In other words, since the transmission line between two resonators is 90° long only at a single frequency, additional reflection zeros appear in measurement. In addtion, fabrication errors that make the transmission line's phase deviate from 90° induce separated reflection zeros at the center frequency.

Non-zero $M_{kk}$ represents that resonator $k$ resonates at different frequency from the center frequency and makes this filter be able to reconfigure its response. For example, by adjusting the resonators 1 and 2, we can obtain a symmetric equi-ripple response. $M_{11} = -M_{22} = \pm 0.184$ results in 20 dB equi-ripple response, and the synthesized and measured results are shown in Fig. 5. Similarly, an asymmetric Butterworth response can be obtained by having non-zero $M_{33}$ and $M_{44}$. Fig. 6 shows the synthesized and measured results for the case of $M_{33} = M_{44} = 0.5$. By using two above-mentioned tuning techniques simultaneously, we may also have asymmetric equi-ripple responses, and one example is shown in Fig. 7. Finally, Fig. 8 shows responses that have two stopbands centered at 3.0, 3.3, and 3.6 GHz, respectively. All responses show good attenuation at stopbands. In conclusion, this filter can suppress various types of spurious and/or interfering signals, which requires adjusting the tuning devices attached to the resonators.

## IV. Conclusion

In this letter, a new dual-stopband filter topology has been proposed. Contrary to the conventional cascaded dual-stopband filters, half of the resonators are coupled to the transmission line in the presented filter topology. It has been shown that the presented filter topology is capable of reconfiguring the frequency response to have asymmetric and/or equi-ripple responses as well as symmetric Butterworth responses. It is worth noting that this filter can reconfigure bandwidths of the stopbands. For validation of the proposed topology, a bandstop filter using substrate-integrated frequency tunable cavity resonators has been designed and fabricated. The approach presented in this letter can be applied to higher-order filter designs.

## References

[1] L. Young, G. L. Matthaei, and E. M. T. Jones, "Microwave band-stop filters with narrow stop bands," *IRE Trans. Microw. Theory Tech.*, vol. 10, no. 6, pp. 416–427, 1962.

[2] D. M. Pozar, *Microwave Engineering 3rd ed.*. New York: Wiley, 2005.

[3] S. Amari and U. Rosenberg, "Direct synthesis of a new class of bandstop filters," *IEEE Trans. Microw. Theory Tech.*, vol. 52, no. 2, pp. 607–616, Feb. 2004.

[4] R. Wu, S. Amari, and U. Rosenberg, "New cross-coupled microstrip band reject filters," *IEEE MTT-S Int. Dig.*, vol. 3, pp. 1597–1600, 2004.

[5] J. Lee, E. J. Naglich, and W. J. Chappell, "Frequency response control in frequency-tunable bandstop filters," *IEEE Microw. Wireless Compon. Lett.*, vol. 20, no. 12, pp. 669–671, Dec. 2010.

[6] J. Lee, E. J. Naglich, H. H. Sigmarsson, D. Peroulis, and W. J. Chappell, "New bandstop filter circuit topology and its application to design of a bandstop-to-bandpass switchable filter," *IEEE Trans. Microw. Theory Tech.*, vol. 61, no. 3, pp. 1114–1123, Mar. 2013.

[7] H. C. Bell, "L-resonator bandstop filters," *IEEE Trans. Microw. Theory Tech.*, vol. 44, no. 12, pp. 2669–2672, Dec. 1996.

[8] J.-S. Hong and M. J. Lancaster, *Microstrip Filter for RF/Microwave Applications*. New York: Wiley, 2001.

[9] E. J. Naglich, J. Lee, D. Peroulis, and W. J. Chappell, "Extended passband bandstop filter cascade with continuous 0.85–6.6-GHz coverage," *IEEE Trans. Microw. Theory Tech.*, vol. 60, no. 1, pp. 21–30, Jan. 2012.

[10] R. J. Cameron, C. M. Kudsia, and R. R. Mansour, *Microwave Filters for Communication Systems: Fundamantals, Design, Applications*. New York: Wiley, 2007.

[11] D. Kajfez and P. Guillon, *Dielectric Resonators*. Norwood, MA: Artech House, Inc., 1986.

[12] S. Amari, U. Rosenberg, and R. Wu, "In-line pseudoelliptic band-reject filters with nonresonating nodes and/or phase shifts," *IEEE Trans. Microw. Theory Tech.*, vol. 54, no. 1, pp. 428–436, Jan. 2006.